Published in final edited form as:
Oncogene. 2014 July 24; 33(30): 3939–3946. doi:10.1038/onc.2013.365.

The MutSβ complex is a modulator of p53-driven tumorigenesis through its functions in both DNA double strand break repair and mismatch repair

Johanna M. M. van Oers, PhD[1], **Yasmin Edwards, PhD**[1], **Richard Chahwan, PhD**[1], **Weijia Zhang, PhD**[2], **Cameron Smith, MSc**[3], **Joaquín Pechuan, BSc**[3], **Sonja Schaetzlein, PhD**[1], **Bo Jin, MD**[1], **Yuxun Wang, MD, PhD**[1], **Aviv Bergman, PhD**[3], **Matthew D. Scharff, MD**[1], and **Winfried Edelmann, PhD**[1]

[1]Department of Cell Biology, Albert Einstein College of Medicine, Bronx, NY 10461

[2]Department of Medicine, Mount Sinai School of Medicine, New York, NY 10029

[3]Department of Systems & Computational Biology, Albert Einstein College of Medicine, Bronx, NY 10461

Abstract

Loss of the DNA mismatch repair protein MSH3 leads to the development of a variety of tumors in mice without significantly affecting survival rates, suggesting a modulating role for the MutSβ (MSH2-MSH3) complex in late onset tumorigenesis. To better study the role of MSH3 in tumor progression, we crossed *Msh3*$^{-/-}$ mice onto a tumor predisposing *p53*-deficient background. Survival of *Msh3/p53* mice was not reduced compared to single *p53* mutant mice; however, the tumor spectrum changed significantly from lymphoma to sarcoma, indicating MSH3 as a potent modulator of p53-driven tumorigenesis. Interestingly, *Msh3*$^{-/-}$ mouse embryonic fibroblasts displayed increased chromatid breaks and persistence of γH2AX foci following ionizing radiation, indicating a defect in DNA double strand break repair. *Msh3/p53* tumors showed increased loss of heterozygosity, elevated genome-wide copy number variation, and a moderate microsatellite instability phenotype compared to *Msh2/p53* tumors, revealing that MSH2-MSH3 suppresses tumorigenesis by maintaining chromosomal stability. Our results show that the MSH2-MSH3 complex is important for the suppression of late onset tumors due to its role in DNA double strand break repair as well as in DNA mismatch repair. Furthermore, they demonstrate that MSH2-MSH3 suppresses chromosomal instability and modulates the tumor spectrum in *p53*-deficient tumorigenesis, and possibly plays a role in other chromosomally unstable tumors as well.

Corresponding author: Winfried Edelmann, Department of Cell Biology, Albert Einstein College of Medicine, 1301 Morris Park Avenue, Bronx, NY 10461, Phone: 718-678-1086, Fax: 718-678-1019, winfried.edelmann@einstein.yu.edu.

Conflict of Interest

The authors declare no conflict of interest.

Supplementary Information accompanies the paper on the Oncogene website (http://www.nature.com/onc)

Keywords

DNA mismatch repair; MSH2-MSH3; DNA double strand break repair; chromosomal instability; p53; sarcomagenesis

Introduction

DNA mismatch repair (MMR) complexes function primarily in the detection and repair of mismatched bases that result from erroneous replication. Two heterodimeric MutS homolog (MSH) complexes, consisting of either MSH2-MSH6 (MutSα) or MSH2-MSH3 (MutSβ), are responsible for the recognition of these mismatched bases. MSH2-MSH6 binds to single base-base mismatches and small insertions/deletions (IDLs), whereas MSH2-MSH3 has a higher affinity for ≥2 base IDLs (1, 2). Germline mutations in *MSH2* and *MSH6* but not *MSH3* are responsible for hereditary non-polyposis colorectal cancer/Lynch syndrome (HNPCC/LS); however, an (A)8 tract in the coding region of *MSH3* was found to be frequently affected by frameshift mutations in MMR-deficient colorectal tumors, resulting in loss of MSH3 protein expression (3). In addition to its role in MMR, yeast studies revealed that during non-conservative homologous recombination, the MSH2-MSH3 complex is required to remove nonhomologous DNA ends during both the initiation of gene conversion and the resolution of single-strand annealing (SSA) intermediates that are initiated by a double strand break (DSB)(4, 5). SSA is a subset of the homologous recombination pathway for repairing spontaneous and induced DSBs that arise between repeated sequences occurring in *cis*. MSH2 and MSH3 recognize and stabilize the nonhomologous 3′ tails at the junction of double-stranded and single-stranded DNA to aid in either the recruitment or cleavage activity of Rad1-Rad10 (6). Although the mechanistic contribution of MSH3 in MMR and DSBR was thought to be overlapping, recent studies have shown that these two MSH3 activities are molecularly distinct (7). MSH2-MSH3 is also involved in triplet repeat (CAG·CTG) expansion diseases such as Huntington and myotonic dystrophy, and it has been shown in several mouse models that MSH2 and MSH3 are absolutely required to generate these expansions (8–12).

Previous observations showed that inactivation of *Msh3* in mice leads to a moderate defect in the repair of insertion/deletion but not base-base mismatches (13), which might explain the absence of *MSH3* mutations in HNPCC/LS families. Among other tumors, *Msh3*$^{-/-}$ mice developed gastrointestinal tumors late in life, which corresponds with loss of MSH3 expression in late onset sporadic colorectal cancer (CRC) in humans (14). In human cancers, loss of MSH3 is associated with an MSI-low (MSI-L) phenotype at dinucleotide repeats and elevated microsatellite alterations at selected tetranucleotide repeats (EMAST) (15, 16). Loss or silencing of *MSH3* also frequently occurs in a variety of other cancers, including non-small cell lung (17), ovarian, bladder (18), and breast (19) cancer. *MSH3* polymorphisms were found to be associated with sporadic colorectal (14, 20, 21), prostate (22), and lung (23) cancer. These findings correlate with a recent report that unlike MutSα, the MutSβ complex is abundant in the majority of mouse tissues (24). Taken together, these studies indicate that MSH2-MSH3 might be important for tumor suppression in multiple tissues and especially in cases of late onset tumorigenesis.

Previous studies in mice showed that loss of *Msh2* is sufficient to initiate and significantly accelerate tumorigenesis, especially in *p53*-deficient mice, and that tumorigenesis is associated with an MSI-high (MSI-H) phenotype (25). The MSH2-MSH6 complex is essential for the repair of base/base mismatches, and loss of either MSH2 or MSH6 therefore results in generation of a severe mutator phenotype and early onset cancers. In contrast, the absence of *MSH3* mutations in early onset HNPCC/LS tumors and the late onset tumor phenotype in $Msh3^{-/-}$ mice indicate that MSH3 is likely not involved in tumor initiation. To determine a possible role for MSH2-MSH3 in tumor progression, we crossed *Msh3* null mice onto the tumor predisposing *p53* null background to create cohorts of both $Msh3^{-/-}p53^{-/-}$ and $Msh3^{-/-}p53^{+/-}$ mice, compared their cancer predisposition phenotype to MMR-deficient *Msh2/p53* mutant mice and analyzed the underlying molecular mechanisms. Although the effects of both *Msh2*- and *Msh3*-deficiency manifest from the earliest stages of life, tumor onset in $Msh3^{-/-}p53^{-/-}$ mice occurred later in life in contrast to the early onset tumorigenesis in $Msh2^{-/-}p53^{-/-}$ mice. We found that due to its role in DSBR rather than MMR, loss of *Msh3* alters the tumor spectrum in *p53* mutant mice by modulating the characteristics of the chromosomal instability (CIN) phenotype, resulting in elevated sarcomagenesis. We conclude that germline mutations in *Msh3* can cause late onset tumorigenesis with various genomic signatures and modulate the tumor spectrum on cancer predisposing backgrounds.

Results

Altered cancer phenotype and elevated sarcomagenesis in *Msh3/p53* mutant mice

To accelerate tumorigenesis in *Msh3* null mice and study tumor progression, we intercrossed $Msh3^{+/-}$ and $p53^{+/-}$ knockout mice and generated two cohorts of mutant mice carrying homozygous mutations in *Msh3* and either homozygous ($Msh3^{-/-}p53^{-/-}$) or heterozygous ($Msh3^{-/-}p53^{+/-}$) mutations in *p53*. To compare loss of *Msh3* to the classic MMR phenotype, additional $Msh2^{-/-}p53^{-/-}$ and $Msh2^{-/-}p53^{+/-}$ cohorts were generated by intercrossing $Msh2^{+/-}$ and $p53^{+/-}$ mice.

$Msh3^{-/-}p53^{-/-}$ double mutant mice showed reduced survival (median survival time 5 months, Figure 1a)when compared with $Msh3^{-/-}$ alone (22 months)(13), but not when compared with $p53^{-/-}$ single mutant mice ($p = .31$, Figure 1a). $Msh3^{-/-}p53^{+/-}$ and $p53^{+/-}$ mice also showed similar survival rates ($p = .11$), suggesting that loss of *Msh3* does not contribute to the initiation or acceleration of tumorigenesis. In contrast, $Msh2^{-/-}p53^{-/-}$ and $Msh2^{-/-}p53^{+/-}$ mice showed significantly reduced survival compared to $p53^{-/-}$ (2 vs. 6 months, $p < .001$) and $p53^{+/-}$ (5 vs. 16 months, $p < .001$) mice respectively, confirming the strong tumorigenic MMR-deficient phenotype that has previously been described for $Msh2^{-/-}$ (26–28), $Msh2^{-/-}p53^{-/-}$ (25), and $Msh2^{-/-}p53^{+/-}$ (29) mice.

The tumor spectrum of $p53^{-/-}$ mice is dominated by lymphomas, but also includes sarcomas and carcinomas (30). Surprisingly, loss of *Msh3* induced a significant shift in the distribution of the various tumor types in *p53* mutant mice: twice as many sarcomas were found in $Msh3^{-/-}p53^{-/-}$ (32% vs. 17%, $p = .04$) and $Msh3^{-/-}p53^{+/-}$ mice (53% vs. 30%, $p = .04$, Figure 1b) compared to tumors from $p53^{-/-}$ and $p53^{+/-}$ mice, respectively. In contrast,

nearly 100% of MMR-deficient *Msh2*$^{-/-}$*p53*$^{-/-}$ and *Msh2*$^{-/-}$*p53*$^{+/-}$ mice succumbed to thymic lymphoma. Only a small number of *Msh3/p53* mice developed gastrointestinal tumors. When tumors were analyzed for their MSI phenotype, which is the hallmark of MMR-deficiency, we found that most tumors from *Msh2*$^{-/-}$*p53*$^{-/-}$ or *Msh2*$^{-/-}$*p53*$^{+/-}$ mice showed MSI at the D7Mit91 and D17Mit123 dinucleotide repeats, compared to few tumors with MSI from *Msh3*$^{-/-}$*p53* mutant mice(Figure 1c). Interestingly, none of the sarcoma samples included in the analysis (0/12) showed MSI. The MSI-L tumor phenotype indicates that defective MMR is not a main mechanism in *Msh3*$^{-/-}$*p53*-driven tumorigenesis.

LOH but not somatic mutation leads to loss of the wild type *p53* allele in *Msh3*$^{-/-}$*p53*$^{+/-}$ tumors

During tumorigenesis, MMR deficiency leads to the accumulation of somatic mutations in tumor suppressor genes and oncogenes. On the other hand, tumors with CIN usually display loss of heterozygosity (LOH) of tumor suppressor genes, which is often associated with defective DSBR pathways(31). Since loss of the tumor suppressor *p53* is a critical event in tumorigenesis, we studied the genetic mechanisms by which the remaining *p53* wild type allele was lost in *Msh3*$^{-/-}$*p53*$^{+/-}$ and *Msh2*$^{-/-}$*p53*$^{+/-}$ tumors. Consistent with the MMR-deficient phenotype, the majority of *Msh2*$^{-/-}$*p53*$^{+/-}$ tumors (63%, 12/19, Table 1) showed mutation of *p53*. All *p53* exons were sequenced, and mutations were found in exons 4, 5, 7, 8, 9, and 11 of *Msh2*$^{-/-}$*p53*$^{+/-}$ tumors. In contrast, no *p53* mutations were detected in the *Msh3*$^{-/-}$*p53*$^{+/-}$ tumors (0/8); however, LOH at the wild type *p53* allele occurred in almost all of the tumors (86%, 6/7) (Figure 1d and Table 1), suggesting a possible role for MSH3 in CIN. LOH of the wild type *p53* allele was also found in some *Msh2*$^{-/-}$*p53*$^{+/-}$ tumors (3/19, 16%), possibly reflecting loss of MSH2-MSH3 function in DSBR.

Msh3-deficient MEFs are defective in DSBR

In yeast, MSH2-MSH3 is involved in the processing of SSA recombination intermediates during certain forms of homologous recombination (5), and loss of this function might result in defective DSBR and contribute to the LOH phenotype in the tumors of *Msh2*$^{-/-}$*p53*$^{+/-}$ and *Msh3*$^{-/-}$*p53*$^{+/-}$ mice. To investigate if mouse MSH3 functions as part of the MSH2-MSH3 complex in the repair of DNA breaks, we first analyzed metaphases of untreated primary mouse embryonic fibroblast (MEF) cell lines. *Msh3*$^{-/-}$ and *Msh2*$^{-/-}$ MEFs both showed a significant increase in chromatid breaks (Figures 2a and 2b), further indicating a defective DSBR response. Since the number of breaks in *Msh6*$^{-/-}$ cells was not significantly different from that in wild type cells ($p = .21$), loss of DSBR appears to be specifically due to the loss of MSH2-MSH3 complex function. Notably, all genotypes showed similar numbers of translocations.

To further analyze the observed DSBR defect, *Msh3*$^{-/-}$ cells were subjected to a low dose of ionizing radiation (1Gy) and efficient resolution of DSBs was subsequently evaluated by counting γH2AX foci in the cell nuclei (Figure 2c). We did not observe a difference in the number of γH2AX foci one hour after irradiation (Figure S1), which suggests that both wild type and *Msh3*$^{-/-}$ MEFs had a comparable accumulation of DSBs at early time-points and that γH2AX signaling is intact in *Msh3*$^{-/-}$ cells. However, two hours after irradiation the majority of wild type cells (95%) showed background levels of 0–10 γH2AX foci per

nucleus in contrast to only 45% of *Msh3*$^{-/-}$ cells (Figure S1). Even 6 hours post-irradiation only 70% of *Msh3*$^{-/-}$ cells were able to adequately resolve DSBs ($p < .001$, Figure 2d), and an increase of more than 10 γH2AX foci per nucleus could be seen in the remaining 30% of nuclei. Taken together, these data demonstrate a moderate DSBR defect in *Msh3*-deficient cells that is revealed by a delay in resolving DSBs.

Msh3 deletion is associated with chromosomal instability in *p53*-deficient tumors

To examine whether loss of MSH3 does lead to chromosomal instability during tumorigenesis, we used spectral karyotyping (SKY) to determine whether lymphomas of *Msh3*-deficient mice displayed any gross chromosomal abnormalities. In contrast to *Msh2*$^{-/-}$*p53*$^{-/-}$ tumor cells, which showed close to normal ploidy (40 chromosomes/cell, Table 2), *Msh3*$^{-/-}$*p53*$^{-/-}$ tumor cell karyotypes showed increased chromosomal instability characterized by significantly increased aneuploidy (55 chromosomes/cell, $p < .001$), translocations, deletions, duplications, and breaks (Figure 3). No specific recurring chromosomal aberrations were found; indicating that loss of MSH3 induces general chromosomal instability. However, the type of chromosomal changes between genotypes tended to be different: *Msh3*$^{-/-}$*p53*$^{-/-}$ and *Msh2*$^{-/-}$*p53*$^{-/-}$ tumor cells showed about two times more translocations compared to *p53*$^{-/-}$ cells (1.2 and 0.9 vs. 0.5 per cell, Table 2), suggesting that the DSBR defect associated with loss of the MSH2-MSH3 complex that was observed earlier contributes to this type of chromosomal rearrangement. In contrast, a trend towards slightly higher numbers of deletions and duplications was observed in *Msh3*$^{-/-}$*p53*$^{-/-}$ and *p53*$^{-/-}$ cells compared to *Msh2*$^{-/-}$*p53*$^{-/-}$ cells, reflecting the aneuploidy phenotype that is associated with the *p53*$^{-/-}$ tumor background.

To study the increase in CIN in *Msh3/p53* tumors in more detail, we used the lymphoma samples that were used for SKY analysis in array comparative genomic hybridization (aCGH) to analyze genome-wide copy number variation (CNV). Since loss of *Msh3* induces sarcomagenesis we also analyzed two groups of *Msh3*$^{-/-}$*p53*$^{+/-}$ and *p53*$^{-/-}$ sarcomas (Figure S2). Again, no increase in CNV was found to recur between samples at specific genomic regions, indicating general chromosomal instability. Compared with *Msh2*$^{-/-}$*p53*$^{-/-}$ lymphoma samples, in which CNV was uncommon, this type of instability was significantly increased in *Msh3*$^{-/-}$*p53*$^{-/-}$ and *p53*$^{-/-}$ lymphomas (Figure 4). Log2 ratio distributions of gains and losses (Figure S3) and subsequent cluster analysis (Figure S4) revealed that both *p53*$^{-/-}$ and *Msh3*$^{-/-}$*p53*$^{-/-}$ lymphomas showed a significant increase in CNV (cluster 1) compared to *Msh2*$^{-/-}$*p53*$^{-/-}$ tumors (cluster 3). *Msh3*$^{-/-}$*p53*$^{-/-}$ and *p53*$^{-/-}$ lymphoma samples clustered together (cluster 1) which indicates that the overall distribution of CNVs throughout the genome in *Msh3*$^{-/-}$*p53*$^{-/-}$ tumors was similar to that of *p53*$^{-/-}$ tumors and that loss of MSH3 does not induce a specific pattern of CNV distribution. Interestingly, the *Msh3/p53* and *p53* sarcoma samples (cluster 2) only showed a moderate increase in CNV compared to *Msh3/p53* and *p53* lymphoma samples. However, the CNV phenotype in *Msh3/p53* sarcomas was significantly more severe than that found in *Msh2/p53* lymphoma samples. Taken together, these results confirm that loss of MSH3, but not MSH2, is associated with an increase in overall chromosomal instability in tumor genomes and that the amount of CIN depends on the underlying predisposing genetic background and the tissue-specific context.

Discussion

The MMR proteins MSH2, MSH6, MLH1 and PMS2 all play a major and well-described role in mismatch repair, and mutations in these genes have been found in patients with HNPCC/LS. Up until now, no mutations have been found in the other MMR proteins MSH3, MLH3 and EXO1 that could directly link them to the development of familial colorectal cancer. Although intestinal tumors developed in *Msh3*(13) and *Mlh3*(32) knockout mice late in life, these proteins appear to have a less pronounced role in MMR and tumor suppression. However, they have been implicated in other processes aside from MMR: apart from their roles in class switch recombination and somatic hypermutation (33–36), MLH3 is essential for processing DSBs at crossovers during meiosis (37), and EXO1 has been identified as a key mediator of DNA end resection during DSBR (38). Surprisingly, it has recently been found that MSH3 protein expression is higher in the majority of murine tissues when compared to MSH6, suggesting important and specific roles for MSH2-MSH3 in DNA repair and genomic instability (24). The similar phenotype of late onset tumors with mild MSI that appeared in $Msh3^{-/-}$ and $Exo1^{-/-}$ mice led us to hypothesize a role for MSH3 in tumor suppression via DSBR and maintenance of chromosomal stability. In this study, we showed that in mice loss of *Msh3* leads to accumulation of unrepaired DSBs, and to a shift in tumor spectrum with increased CIN on a *p53*-driven tumor predisposing background.

As described before (25), mice with combined *Msh2* and *p53* ablation show independent segregation of the MSI phenotype compared to $p53^{-/-}$ alone, which suggests that loss of *Msh2* is dominant over the $p53^{-/-}$ phenotype. Furthermore, their synergism in tumorigenesis suggests that they are not genetically epistatic. In contrast, $Msh3^{-/-}p53^{-/-}$ mice show features that are more similar to the $p53^{-/-}$ phenotype. The lack of synergism in tumorigenesis and the shift in tumor spectrum towards sarcomagenesis suggest that MSH3 might not be involved in tumor initiation but rather in tumor progression by modulating the *p53*-deficient phenotype. Interestingly, loss of *p53* did not accelerate gastrointestinal tumorigenesis of $Msh3^{-/-}$ mice since we only detected a small number of gastrointestinal carcinomas in *Msh3/p53* mutant mice (Figure 1b). Since loss of MSH3 is associated with a variety of human cancer types, its effects might be evident on other predisposing backgrounds, implicating MSH3 as a general modulator of cancer phenotypes. The contribution of *Msh3* deletion to tumorigenesis, however, depends on the genetic context and subsequent mechanism of tumorigenesis in different tissues, since $Msh3^{-/-}Apc^{1638N}$ mice did not show a different tumor onset or phenotype compared to Apc^{1638N} mice (39).

Due to the strong aneuploidy phenotype caused by loss of *p53*(40, 41) it was not immediately clear whether loss of Msh3 contributed to the increase in CIN in $Msh3^{-/-}p53^{-/-}$ tumors. However, although there were not enough tumor samples available for SKY analysis, we observed differences between tumors with combined *Msh3/p53* deficiency and single *p53* deficiency with a trend towards an increase in the average number of translocations per cell for $Msh3^{-/-}p53^{-/-}$ tumors compared to $p53^{-/-}$ alone, indicating defective DSBR caused by loss of the MSH2-MSH3 complex in these tumors. This defect in DSBR was also visible when we counted chromosomal aberrations in metaphase spreads, showing a significant increase in chromatid breaks in $Msh3^{-/-}$ and $Msh2^{-/-}$ MEFs.

Interestingly, here the number of translocations was not significantly different between wild type, *Msh3*$^{-/-}$ and *Msh2*$^{-/-}$ MEFs, which might be due to technical difficulties with scoring translocations in regular metaphase spreads. Alternatively, this data suggests that loss of MSH2-MSH3-dependent DSBR results in an increase in the number of translocations during the clonal outgrowth of *p53*-deficient tumors and contributes to *p53*-driven tumorigenesis. The amount of chromosomal instability represented by CNV, however, is significantly increased in *Msh3*$^{-/-}$*p53*$^{+/-}$ tumors (Figure 4 and Figure S2) compared to the CNV phenotype in *p53*$^{+/-}$ tumors from our previous study (48) which indicates that loss of *Msh3* is contributing to the chromosomal instability phenotype in *Msh3*$^{-/-}$*p53*$^{+/-}$ tumors.

Our observations indicate a dual function for the MutSβ complex in genome maintenance and tumor suppression (Figure 5). *Msh2*-deficient mice display a strong MMR defect with accumulation of mutations and low chromosomal instability, indicating the essential role for MSH2 in MMR. On the other hand, a moderate DSBR defect is associated with the loss of either MSH2 or MSH3, and whereas the mild phenotypes with regard to CIN and tumorigenesis that are associated with the loss of MSH2-MSH3 dependent DSBR are difficult to observe in the dominant MMR tumor phenotype of *Msh2*-deficient mice, we were able to study them by deleting *Msh3* on the appropriate tumor predisposing background. Because the DSBR defect is not as severe as the defect caused by loss of other canonical DSBR proteins, this further suggests a role for MSH3 in the repair of a subset of DSBs, possibly substrates of the SSA pathway (6, 7). Interestingly, loss of MSH3 was shown to be associated with accelerated tumor progression in MLH1-deficient colorectal cancers, and it was suggested that the effect of MSH3 loss on tumor progression might be related to another function of MSH3 unrelated to MMR, implicating its role in DNA DSBR by SSA (3). It remains unclear whether the role of MSH3 in DSBR is dependent on its recruitment via the MMR pathway, either during the process of homeologous recombination or when small IDLs or DNA mismatches (42) on opposite strands are in close proximity so as to mediate the formation of DSBs during the MMR process, or whether MSH2-MSH3 could instead be recruited directly to sites of DSBs. Regardless, MSH3 was shown to co-localize with γH2AX and DSB foci following genotoxic stress (43, 44), which suggests that it might be directly involved in a subset of DSBR events.

Despite the moderate defect in DSBR *Msh3* deficient mice showed a significant increase in sarcomagenesis, suggesting that loss of MSH3 targets sarcoma tumor suppressor genes and modulates *p53*-dependent tumorigenesis. When we analyzed lymphomas and sarcomas for genomic instability, *Msh3*$^{-/-}$*p53*$^{-/-}$ and *p53*$^{-/-}$ lymphomas showed the largest increase in CNV while *Msh2*$^{-/-}$*p53*$^{-/-}$ mice displayed a low CNV phenotype. Interestingly, both *Msh3/p53* and *p53* sarcomas displayed significantly more CNV than *Msh2/p53* lymphomas, but less CNV than *Msh3/p53* and *p53* lymphomas, and clustered together based on their moderate CNV profile. This indicates that loss of *Msh3* causes a repair defect that contributes to genomic instability in a tissue-specific manner and promotes *p53*-driven sarcomagenesis. Since the sarcomas in our mouse cohorts are microsatellite stable, the increase in sarcoma incidence in *Msh3/p53* mutant mice is likely caused by loss of Msh3-dependent DSBR which contributes to the moderate CIN that is associated with sarcomagenesis. However, loss of Msh3-dependent MMR might also play a role in *p53*-

dependent sarcomagenesis by resulting in a low-level mutator phenotype that might be difficult to detect (2, 42).

In conclusion, our data indicate for the first time that the MSH2-MSH3 protein complex is involved in tumorigenesis through maintenance of chromosomal stability. In contrast to the MutSα complex (MSH2-MSH6), which has a dominant role in genome maintenance by MMR, MSH2-MSH3 functions both in MMR, indicated by an MSI-L phenotype, and DSBR, as has been recently shown in yeast (7). Loss of MSH3 can therefore contribute to tumorigenesis in two ways: by a mild MMR defect leading to MSI-L and low-level mutation accumulation, and by a DSBR defect that leads to a moderate increase in CIN. Since most sporadic colorectal cancers (CRCs) are CIN (85%) (45), the MSH2-MSH3 complex might play an important role in suppression of late-onset sporadic cancers that are MSI-L. Future studies should therefore include the analysis of *Msh3* loss on multiple tumorigenic backgrounds to assess a more specific role for MSH3 in tumorigenesis.

Materials and methods

Animals, tumors and survival

Msh2$^{-/-}$, *Msh3*$^{-/-}$ and *Msh6*$^{-/-}$ knockout mice were previously generated in our lab (13, 28, 46). *p53*$^{-/-}$ knockout mice (47) were purchased from Jackson Laboratories. All mice were on a congenic C57BL/6 background. Mice were intercrossed as described and observed until they became morbid or moribund. Tumors were removed and fixed in 10% buffered formalin or frozen at −150°C. After paraffin embedding of fixed tissue, sections were stained with hematoxylin and eosin. Statistical analysis of tumor incidence was completed with IBM SPSS Statistics version 20.0 (IBM Corp., Armonk, NY). The Kaplan-Meier method was used to compare curves for survival, with significance evaluated by two-sided log rank statistics. A Chi squared test was used to assess the influence of genotype on the tumor spectrum.

Microsatellite instability, LOH, and mutational analysis of *p53*

For MSI analysis, the D7Mit91 and D17Mit123 microsatellite loci were amplified from normal and tumor DNA and analyzed as previously described (39). Tumor DNA was also serially diluted and analyzed for loss of the wild type *p53* allele as previously described (48). To analyze tumors for *p53* mutations, primers amplifying all exons of *p53* (including both transcript variants of exon 11) were used as described (49), followed by DNA sequencing.

Chromatid break and double strand break analysis

Primary mouse embryonic fibroblasts (MEFs, p4–6) were treated overnight with 0.1 μg/ml colcemid (Invitrogen, Carlsbad, CA) and subsequently swelled, fixed, and dropped onto glass slides to prepare metaphase spreads. DNA was stained using mounting medium with DAPI (Vector Laboratories, Inc., Burlingame, CA), and at least 100 metaphases in 2–3 different cell lines were analyzed per genotype.

For DSB analysis, MEFs were cultured on poly-L-lysine coated slides (Sigma, St. Louis, MO), irradiated with 1 Gy, and incubated at 37°C for 30 min – 6h. Cells were fixed with cold 1:1 methanol:acetone for 5 min, and washed twice with cold PBS for 5 min. After blocking with 10% FBS in PBS, cells were incubated overnight with a mouse monoclonal γH2AX antibody (Upstate, Billerica, MA; 1:500). Cells were again washed twice in cold PBS for 5 min, and incubated for 1h at room temperature with an Alexa Fluor 488-labeled goat anti-mouse antibody (Invitrogen). DNA was stained using mounting medium with DAPI. The experiment was repeated three times for two different cell lines per genotype, and a minimum of 100 cells was analyzed each time.

Metaphases and foci were counted using an Olympus BX61 microscope (Olympus America Inc., Center Valley, PA) with Sensicam QE cooled CCD camera (PCO, Kelheim, Germany). Significant differences between cell lines in the number of breaks or γH2AX foci were calculated using an independent two sample *t* test of equal variance.

Spectral karyotyping (SKY)

Thymic lymphomas were dissociated, filtered, and resuspended as described (50). To prepare metaphase spreads, cells were treated with colcemid for 3–6 hours, swelled, fixed, and dropped onto clean glass slides inside a humidity chamber. SKY was performed as previously described (51). Slides were hybridized with the combinatorially labeled whole chromosome painting probes (Applied Spectral Imaging, Inc., Carlsbad, CA) and metaphase images were captured using the Applied Spectral Imaging interferometer on an epifluorescence microscope (Zeiss). SKY karyotypes were then analyzed with SkyView™ version 1.62 (Applied Spectral Imaging, Inc.). Metaphases were captured and analyzed using the nomenclature approved by the International Committee on Standardized Genetic Nomenclature for Mice (http://www.informatics.jax.org).

Array comparative genomic hybridization (aCGH)

Genomic DNA was isolated from frozen tumor tissue and matched normal tail tissue using the Qiagen DNeasy kit, and hybridized to NimbleGen Mouse CGH 3×720K Whole-Genome Tiling Arrays (Roche NimbleGen, Inc., Madison, WI) in four different experiments. To represent the wide variation of mouse sarcoma samples but also to homogenize between genotypes, groups were composed of one fibrohistiocytic, one hemangio- and one spindle cell sarcoma each.

Plotting summaries of copy number changes among all samples for each genotype was done as described before (48). In order to compare copy number changes between different sets of samples, distributions of the (log2) ratios for the segmented data were plotted for each sample. The tails of this distribution (weight) were used to indicate the amount of chromosomal instability: That is, for each distribution, the proportion of data points >3 s.d. of the distribution with the lowest variance was computed on the left and right tails, i.e. relative copy number increase (gain) or decrease (loss) according to the aCGH data. Samples were subsequently clustered using the k-means clustering algorithm. Consistency of the clusters obtained was evaluated by the silhouette method(52).

Supplementary Material

Refer to Web version on PubMed Central for supplementary material.

Acknowledgments

We thank Rani Sellers from the Einstein Histotechnology and Comparative Pathology facility for mouse pathology and for reviewing the manuscript. This study was supported by National Institutes of Health grants CA76329 and CA93484 (WE), and CA72649 and CA102705 (MDS). MDS is supported by the Harry Eagle Chair provided by the National Women's Division of the Albert Einstein College of Medicine.

References

1. Iyer RR, Pluciennik A, Burdett V, Modrich PL. DNA mismatch repair: functions and mechanisms. Chem Rev. 2006; 106(2):302–23. [PubMed: 16464007]
2. Marsischky GT, Kolodner RD. Biochemical characterization of the interaction between the Saccharomyces cerevisiae MSH2-MSH6 complex and mispaired bases in DNA. The Journal of biological chemistry. 1999; 274(38):26668–82. [PubMed: 10480869]
3. Plaschke J, Kruger S, Jeske B, Theissig F, Kreuz FR, Pistorius S, et al. Loss of MSH3 protein expression is frequent in MLH1-deficient colorectal cancer and is associated with disease progression. Cancer research. 2004; 64(3):864–70. Epub 2004/02/12. [PubMed: 14871813]
4. Evans E, Sugawara N, Haber JE, Alani E. The Saccharomyces cerevisiae Msh2 mismatch repair protein localizes to recombination intermediates in vivo. Molecular cell. 2000; 5(5):789–99. Epub 2000/07/06. [PubMed: 10882115]
5. Sugawara N, Paques F, Colaiacovo M, Haber JE. Role of Saccharomyces cerevisiae Msh2 and Msh3 repair proteins in double-strand break-induced recombination. Proceedings of the National Academy of Sciences of the United States of America. 1997; 94(17):9214–9. Epub 1997/08/19. [PubMed: 9256462]
6. Lyndaker AM, Alani E. A tale of tails: insights into the coordination of 3′ end processing during homologous recombination. Bioessays. 2009; 31(3):315–21. Epub 2009/03/05. [PubMed: 19260026]
7. Kumar C, Williams GM, Havens B, Dinicola M, Surtees JA. Distinct requirements within the Msh3 nucleotide binding pocket for mismatch and double-strand break repair. Journal of molecular biology. 2013 Epub 2013/03/06.
8. Manley K, Shirley TL, Flaherty L, Messer A. Msh2 deficiency prevents in vivo somatic instability of the CAG repeat in Huntington disease transgenic mice. Nature genetics. 1999; 23(4):471–3. Epub 1999/12/02. [PubMed: 10581038]
9. Owen BA, Yang Z, Lai M, Gajec M, Badger JD 2nd, Hayes JJ, et al. (CAG)(n)-hairpin DNA binds to Msh2-Msh3 and changes properties of mismatch recognition. Nat Struct Mol Biol. 2005; 12(8): 663–70. Epub 2005/07/19. [PubMed: 16025128]
10. Savouret C, Brisson E, Essers J, Kanaar R, Pastink A, te Riele H, et al. CTG repeat instability and size variation timing in DNA repair-deficient mice. EMBO J. 2003; 22(9):2264–73. Epub 2003/05/03. [PubMed: 12727892]
11. van den Broek WJ, Nelen MR, Wansink DG, Coerwinkel MM, te Riele H, Groenen PJ, et al. Somatic expansion behaviour of the (CTG)n repeat in myotonic dystrophy knock-in mice is differentially affected by Msh3 and Msh6 mismatch-repair proteins. Hum Mol Genet. 2002; 11(2): 191–8. Epub 2002/01/26. [PubMed: 11809728]
12. Tome S, Holt I, Edelmann W, Morris GE, Munnich A, Pearson CE, et al. MSH2 ATPase domain mutation affects CTG*CAG repeat instability in transgenic mice. PLoS genetics. 2009; 5(5):e1000482. [PubMed: 19436705]
13. Edelmann W, Umar A, Yang K, Heyer J, Kucherlapati M, Lia M, et al. The DNA mismatch repair genes Msh3 and Msh6 cooperate in intestinal tumor suppression. Cancer research. 2000; 60(4): 803–7. Epub 2000/03/08. [PubMed: 10706084]

14. Plaschke J, Preussler M, Ziegler A, Schackert HK. Aberrant protein expression and frequent allelic loss of MSH3 in colorectal cancer with low-level microsatellite instability. Int J Colorectal Dis. 2012; 27(7):911–9. Epub 2012/01/18. [PubMed: 22249440]
15. Haugen AC, Goel A, Yamada K, Marra G, Nguyen TP, Nagasaka T, et al. Genetic instability caused by loss of MutS homologue 3 in human colorectal cancer. Cancer research. 2008; 68(20): 8465–72. Epub 2008/10/17. [PubMed: 18922920]
16. Lee SY, Chung H, Devaraj B, Iwaizumi M, Han HS, Hwang DY, et al. Microsatellite alterations at selected tetranucleotide repeats are associated with morphologies of colorectal neoplasias. Gastroenterology. 2010; 139(5):1519–25. Epub 2010/08/17. [PubMed: 20708618]
17. Benachenhou N, Guiral S, Gorska-Flipot I, Labuda D, Sinnett D. High resolution deletion mapping reveals frequent allelic losses at the DNA mismatch repair loci hMLH1 and hMSH3 in non-small cell lung cancer. International journal of cancer. 1998; 77(2):173–80. Epub 1998/07/03.
18. Kawakami T, Shiina H, Igawa M, Deguchi M, Nakajima K, Ogishima T, et al. Inactivation of the hMSH3 mismatch repair gene in bladder cancer. Biochemical and biophysical research communications. 2004; 325(3):934–42. Epub 2004/11/16. [PubMed: 15541380]
19. Benachenhou N, Guiral S, Gorska-Flipot I, Labuda D, Sinnett D. Frequent loss of heterozygosity at the DNA mismatch-repair loci hMLH1 and hMSH3 in sporadic breast cancer. British journal of cancer. 1999; 79(7–8):1012–7. Epub 1999/03/31. [PubMed: 10098729]
20. Berndt SI, Platz EA, Fallin MD, Thuita LW, Hoffman SC, Helzlsouer KJ. Mismatch repair polymorphisms and the risk of colorectal cancer. International journal of cancer. 2007; 120(7): 1548–54. Epub 2007/01/06.
21. Orimo H, Nakajima E, Yamamoto M, Ikejima M, Emi M, Shimada T. Association between single nucleotide polymorphisms in the hMSH3 gene and sporadic colon cancer with microsatellite instability. J Hum Genet. 2000; 45(4):228–30. Epub 2000/08/17. [PubMed: 10944853]
22. Hirata H, Hinoda Y, Kawamoto K, Kikuno N, Suehiro Y, Okayama N, et al. Mismatch repair gene MSH3 polymorphism is associated with the risk of sporadic prostate cancer. J Urol. 2008; 179(5): 2020–4. Epub 2008/03/22. [PubMed: 18355840]
23. Michiels S, Danoy P, Dessen P, Bera A, Boulet T, Bouchardy C, et al. Polymorphism discovery in 62 DNA repair genes and haplotype associations with risks for lung and head and neck cancers. Carcinogenesis. 2007; 28(8):1731–9. Epub 2007/05/12. [PubMed: 17494052]
24. Tome S, Simard JP, Slean MM, Holt I, Morris GE, Wojciechowicz K, et al. Tissue-specific mismatch repair protein expression: MSH3 is higher than MSH6 in multiple mouse tissues. DNA repair. 2013; 12(1):46–52. Epub 2012/12/12. [PubMed: 23228367]
25. Cranston A, Bocker T, Reitmair A, Palazzo J, Wilson T, Mak T, et al. Female embryonic lethality in mice nullizygous for both Msh2 and p53. Nature genetics. 1997; 17(1):114–8. [PubMed: 9288110]
26. Reitmair AH, Schmits R, Ewel A, Bapat B, Redston M, Mitri A, et al. MSH2 deficient mice are viable and susceptible to lymphoid tumours. Nature genetics. 1995; 11(1):64–70. [PubMed: 7550317]
27. de Wind N, Dekker M, Berns A, Radman M, te Riele H. Inactivation of the mouse Msh2 gene results in mismatch repair deficiency, methylation tolerance, hyperrecombination, and predisposition to cancer. Cell. 1995; 82(2):321–30. Epub 1995/07/28. [PubMed: 7628020]
28. Smits R, Hofland N, Edelmann W, Geugien M, Jagmohan-Changur S, Albuquerque C, et al. Somatic Apc mutations are selected upon their capacity to inactivate the beta-catenin downregulating activity. Genes Chromosomes Cancer. 2000; 29(3):229–39. Epub 2000/09/19. [PubMed: 10992298]
29. Toft NJ, Curtis LJ, Sansom OJ, Leitch AL, Wyllie AH, te Riele H, et al. Heterozygosity for p53 promotes microsatellite instability and tumorigenesis on a Msh2 deficient background. Oncogene. 2002; 21(41):6299–306. Epub 2002/09/06. [PubMed: 12214270]
30. Jacks T. Lessons from the p53 mutant mouse. Journal of cancer research and clinical oncology. 1996; 122(6):319–27. [PubMed: 8642041]
31. Miura T, Yamana Y, Usui T, Ogawa HI, Yamamoto MT, Kusano K. Homologous recombination via synthesis-dependent strand annealing in yeast requires the Irc20 and Srs2 DNA helicases. Genetics. 2012; 191(1):65–78. Epub 2012/03/01. [PubMed: 22367032]

32. Chen PC, Dudley S, Hagen W, Dizon D, Paxton L, Reichow D, et al. Contributions by MutL homologues Mlh3 and Pms2 to DNA mismatch repair and tumor suppression in the mouse. Cancer research. 2005; 65(19):8662–70. [PubMed: 16204034]
33. Bardwell PD, Woo CJ, Wei K, Li Z, Martin A, Sack SZ, et al. Altered somatic hypermutation and reduced class-switch recombination in exonuclease 1-mutant mice. Nat Immunol. 2004; 5(2):224–9. [PubMed: 14716311]
34. Li Z, Peled JU, Zhao C, Svetlanov A, Ronai D, Cohen PE, et al. A role for Mlh3 in somatic hypermutation. DNA repair. 2006; 5(6):675–82. [PubMed: 16564751]
35. Li Z, Scherer SJ, Ronai D, Iglesias-Ussel MD, Peled JU, Bardwell PD, et al. Examination of Msh6- and Msh3-deficient mice in class switching reveals overlapping and distinct roles of MutS homologues in antibody diversification. J Exp Med. 2004; 200(1):47–59. Epub 2004/07/09. [PubMed: 15238604]
36. Wu X, Tsai CY, Patam MB, Zan H, Chen JP, Lipkin SM, et al. A role for the MutL mismatch repair Mlh3 protein in immunoglobulin class switch DNA recombination and somatic hypermutation. J Immunol. 2006; 176(9):5426–37. [PubMed: 16622010]
37. Svetlanov A, Baudat F, Cohen PE, de Massy B. Distinct functions of MLH3 at recombination hot spots in the mouse. Genetics. 2008; 178(4):1937–45. Epub 2008/04/24. [PubMed: 18430927]
38. Tomimatsu N, Mukherjee B, Deland K, Kurimasa A, Bolderson E, Khanna KK, et al. Exo1 plays a major role in DNA end resection in humans and influences double-strand break repair and damage signaling decisions. DNA repair. 2012; 11(4):441–8. Epub 2012/02/14. [PubMed: 22326273]
39. Kuraguchi M, Yang K, Wong E, Avdievich E, Fan K, Kolodner RD, et al. The distinct spectra of tumor-associated Apc mutations in mismatch repair-deficient Apc1638N mice define the roles of MSH3 and MSH6 in DNA repair and intestinal tumorigenesis. Cancer research. 2001; 61(21): 7934–42. Epub 2001/11/03. [PubMed: 11691815]
40. Fukasawa K, Choi T, Kuriyama R, Rulong S, Vande Woude GF. Abnormal centrosome amplification in the absence of p53. Science. 1996; 271(5256):1744–7. Epub 1996/03/22. [PubMed: 8596939]
41. Tomasini R, Mak TW, Melino G. The impact of p53 and p73 on aneuploidy and cancer. Trends Cell Biol. 2008; 18(5):244–52. Epub 2008/04/15. [PubMed: 18406616]
42. Harrington JM, Kolodner RD. Saccharomyces cerevisiae Msh2-Msh3 acts in repair of base-base mispairs. Molecular and cellular biology. 2007; 27(18):6546–54. Epub 2007/07/20. [PubMed: 17636021]
43. Hong Z, Jiang J, Hashiguchi K, Hoshi M, Lan L, Yasui A. Recruitment of mismatch repair proteins to the site of DNA damage in human cells. J Cell Sci. 2008; 121(Pt 19):3146–54. Epub 2008/09/04. [PubMed: 18765568]
44. Reynolds MF, Peterson-Roth EC, Bespalov IA, Johnston T, Gurel VM, Menard HL, et al. Rapid DNA double-strand breaks resulting from processing of Cr-DNA cross-links by both MutS dimers. Cancer research. 2009; 69(3):1071–9. Epub 2009/01/15. [PubMed: 19141647]
45. Pino MS, Chung DC. The chromosomal instability pathway in colon cancer. Gastroenterology. 2010; 138(6):2059–72. Epub 2010/04/28. [PubMed: 20420946]
46. Edelmann W, Yang K, Umar A, Heyer J, Lau K, Fan K, et al. Mutation in the mismatch repair gene Msh6 causes cancer susceptibility. Cell. 1997; 91(4):467–77. [PubMed: 9390556]
47. Jacks T, Remington L, Williams BO, Schmitt EM, Halachmi S, Bronson RT, et al. Tumor spectrum analysis in p53-mutant mice. Current biology: CB. 1994; 4(1):1–7. Epub 1994/01/01. [PubMed: 7922305]
48. Wang Y, Zhang W, Edelmann L, Kolodner RD, Kucherlapati R, Edelmann W. Cis lethal genetic interactions attenuate and alter p53 tumorigenesis. Proceedings of the National Academy of Sciences of the United States of America. 2010; 107(12):5511–5. Epub 2010/03/10. [PubMed: 20212136]
49. Varela I, Klijn C, Stephens PJ, Mudie LJ, Stebbings L, Galappaththige D, et al. Somatic structural rearrangements in genetically engineered mouse mammary tumors. Genome Biol. 2010; 11(10):R100. Epub 2010/10/15. [PubMed: 20942901]

50. Peled JU, Sellers RS, Iglesias-Ussel MD, Shin DM, Montagna C, Zhao C, et al. Msh6 protects mature B cells from lymphoma by preserving genomic stability. Am J Pathol. 2010; 177(5):2597–608. Epub 2010/10/12. [PubMed: 20934970]

51. Schrock E, du Manoir S, Veldman T, Schoell B, Wienberg J, Ferguson-Smith MA, et al. Multicolor spectral karyotyping of human chromosomes. Science. 1996; 273(5274):494–7. Epub 1996/07/26. [PubMed: 8662537]

52. Rousseeuw PJ. Silhouettes: A graphical aid to the interpretation and validation of cluster analysis. Journal of Computational and Applied Mathematics. 1987; 20:53–65.

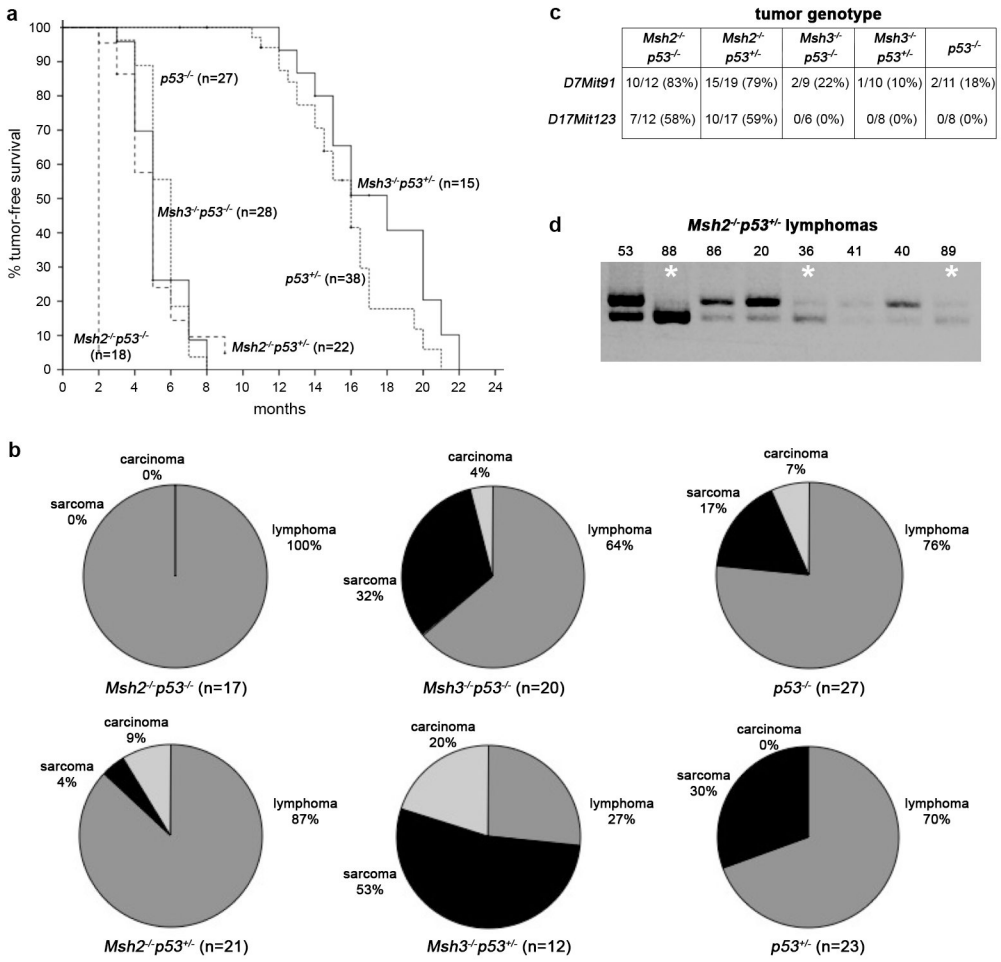

Figure 1.

Loss of *Msh3* modifies tumor phenotype of *p53* null mice. (**a**) Tumor-free survival was significantly different for $Msh2^{-/-}p53^{-/-}$ and $p53^{-/-}$ mice ($p < .001$) and for $Msh2^{-/-}p53^{+/-}$ and $p53^{+/-}$ mice ($p < .001$). In contrast, survival was similar for$Msh3^{-/-}p53^{-/-}$ and $p53^{-/-}$ mice ($p = .31$) and for $Msh3^{-/-}p53^{+/-}$ and $p53^{+/-}$ mice ($p = .11$). Dashed lines, *Msh2/p53* genotypes; solid lines, *Msh3/p53* genotypes; dotted lines, single *p53* genotypes. (**b**) Tumor type and incidence in mice with different *Msh2*, *Msh3*, and *p53* genotypes. The percentage of sarcomas is increased in $Msh3^{-/-}p53^{-/-}$ and $Msh3^{-/-}p53^{+/-}$ mice compared to $p53^{-/-}$ and $p53^{+/-}$ mice, respectively ($p = .04$). Also, the carcinoma phenotype includes a small number of small intestinal tumors ($Msh3^{-/-}p53^{-/-}$, 1; $Msh3^{-/-}p53^{+/-}$, 2). (**c**) Microsatellite instability (MSI) analysis of tumors at the dinucleotide loci D7Mit91 and D17Mit123, determined by the number of unstable alleles divided by the total number of alleles scored. (**d**) Loss of heterozygosity (LOH) of the wild type p53 allele (*) was demonstrated in $Msh2^{-/-}p53^{+/-}$ or $Msh3^{-/-}p53^{+/-}$ tumor samples using PCR (see also Table 1). Upper band, wild type allele (540 bp); lower band, *p53* null allele (480 bp).

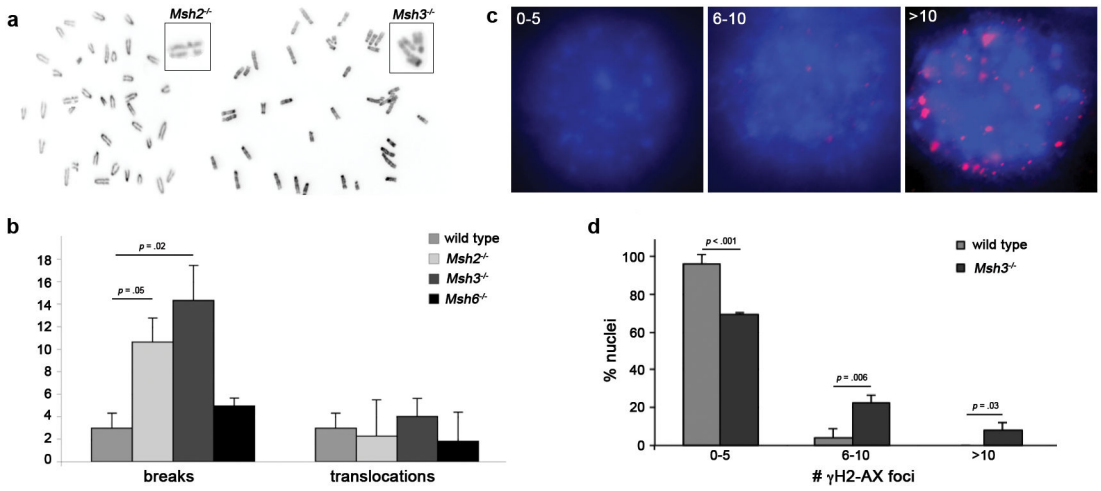

Figure 2.

Loss of *Msh3* induces a double strand break repair defect. (**a**) Metaphase spreads from *Msh2*$^{-/-}$ (left) and *Msh3*$^{-/-}$ (right) mouse embryonic fibroblasts (MEFs). Examples of chromatid breaks are magnified in insets. (**b**) Chromosomal aberrations were analyzed for >100 metaphase nuclei per genotype in MEF cell lines. Average numbers of chromatid breaks and translocations are shown. (**c**) Three categories of γH2AX foci accumulation were defined after staining with DAPI (blue) and anti-γH2AX antibody (red): 0–5, 6–10, and >10 foci per nucleus. (**d**) Deficient double strand break repair was defined by accumulation of γH2AX foci in *Msh3*$^{-/-}$ and wild type MEFs 6h after irradiation with 1Gy.

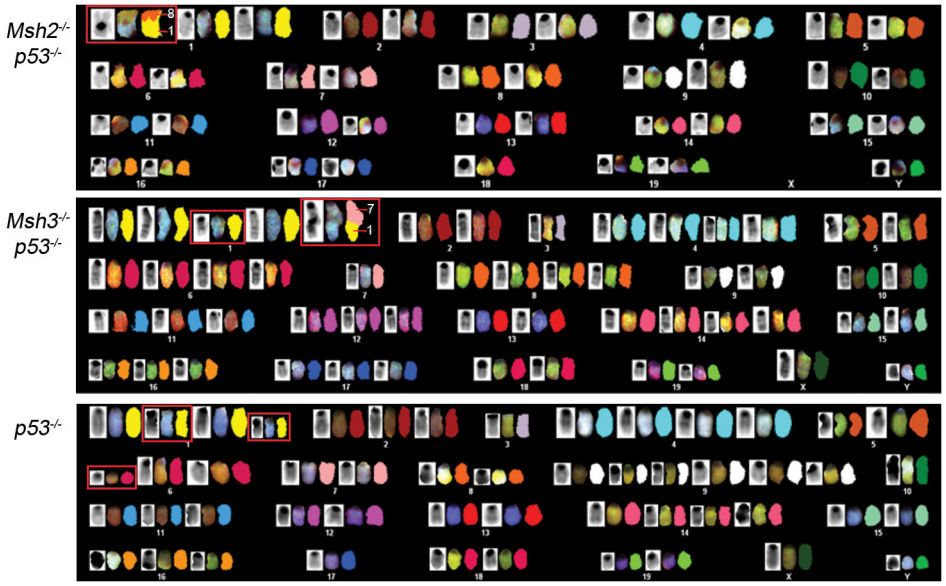

Figure 3.

MSH3 is involved in maintaining chromosomal stability. Examples of spectral karyotypes from lymphoma cells are shown for each genotype, indicating a close to normal karyotype and t(1,8) for *Msh2*$^{-/-}$*p53*$^{-/-}$, increased aneuploidy, del1, and t(1,7) for *Msh3*$^{-/-}$*p53*$^{-/-}$, and increased aneuploidy, 2del1 and del6 for *p53*$^{-/-}$. Red boxes indicate translocations and deletions.

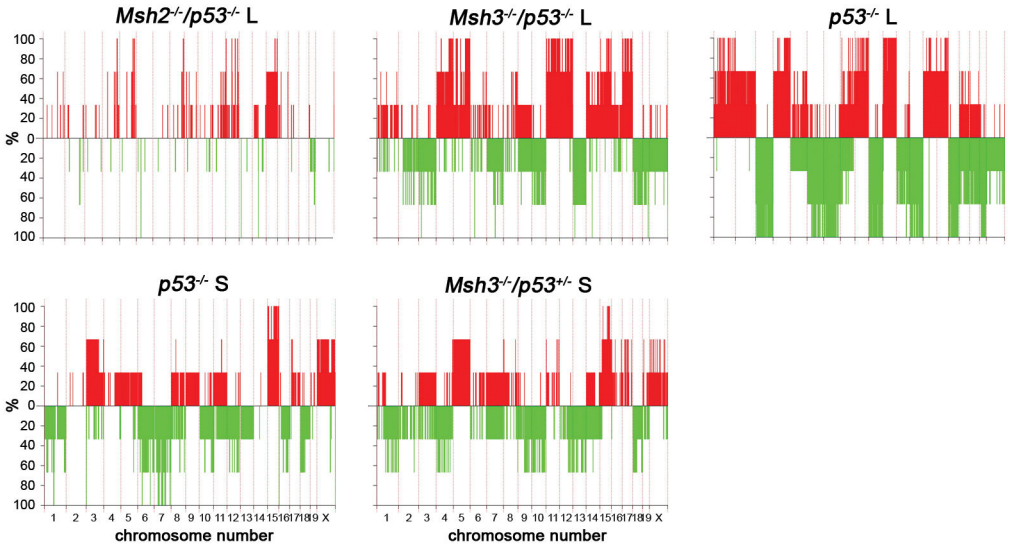

Figure 4.

Loss of *Msh3* is associated with a high level of CNV. Chromosome copy number changes were analyzed as described before (48). To account for tumor heterogeneity, large segments with low-level copy number changes were considered as important as small segments with high-level changes, and no arbitrary log2 ratio was used. %, percentage of samples that showed gain (red) or loss (green). L, lymphoma; S, sarcoma.

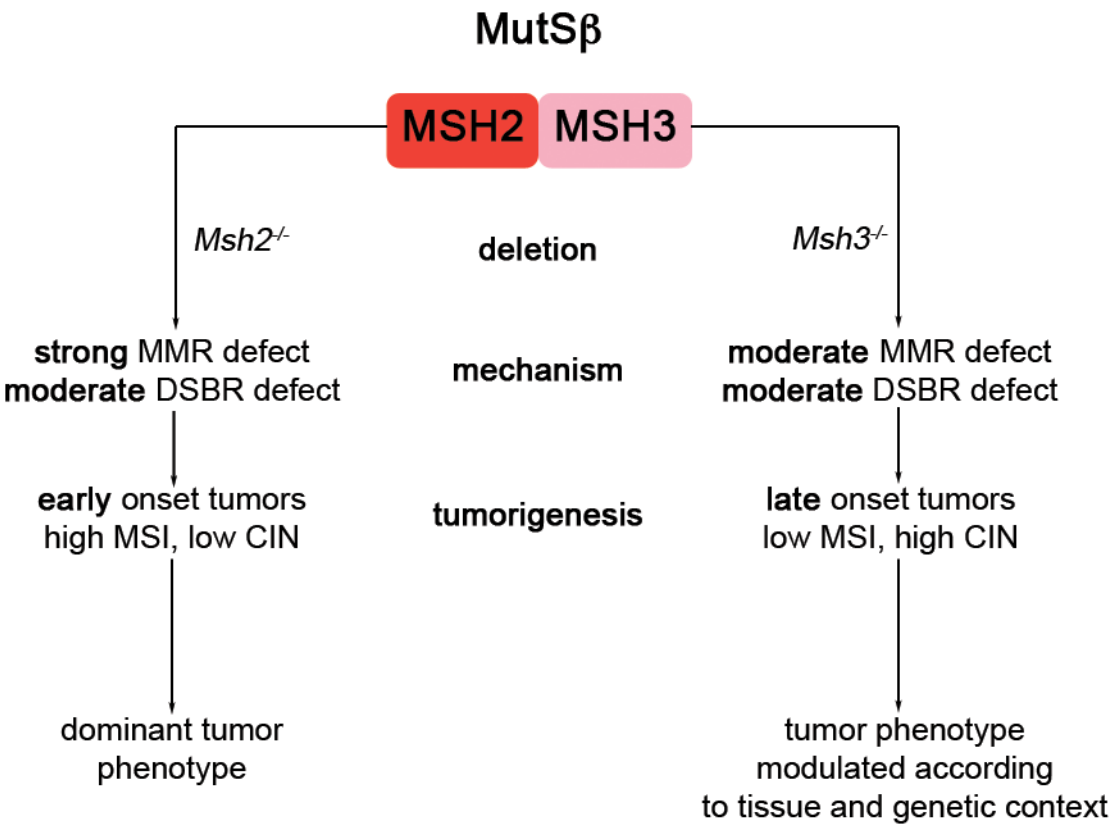

Figure 5.

Model representing the different functions of the Mutsβ (MSH2-MSH3) complex. Deletion of *Msh2* induces a strong MMR defect and a moderate DSBR defect, leading to a dominant tumor phenotype with early onset tumors that are MSI-high and chromosomally stable. Deletion of *Msh3* revealed a moderate DSBR defect next to the previously described moderate MMR defect, resulting in a modulated tumor phenotype of late onset tumors that were MSI-low and showed increased chromosomal instability.

Table 1

p53 mutation and LOH in $p53^{+/-}$ tumors

Tumor sample	exon 4	exon 5	exon 7	exon 8	exon 9	exon 11.1	LOH
$Msh2^{-/-}p53^{+/-}$							
29						$del\ (A)_7$	
47						$del\ (A)_7$	
90							
66I	$ins\ (T)_6$						
73	Q112STOP						
65							null
49							
48					$del\ (C)_5$		
66II	ND[a]			$del\ (A)_5$	ND	ND	
63	ND			$del\ (C)_5$	ND	ND	
53	ND		$del\ (G)_6$		ND	ND	
88	ND	Q141STOP			ND	ND	wt
86	ND			$del\ (A)_5$	ND	ND	
20							
36							wt
41	ND			$del\ (C)_5$	ND	ND	
40	ND		$del\ (G)_6$		ND	ND	
89							wt
14							
$Msh3^{-/-}p53^{+/-}$							
43	ND				ND	ND	wt
42	ND				ND	ND	wt
45	ND				ND	ND	wt
56	ND				ND	ND	ND
66	ND				ND	ND	wt
54	ND	ND			ND	ND	ND

Tumor sample	exon 4	exon 5	exon 7	exon 8	exon 9	exon 11.1	LOH
36							
64	ND	ND			ND	ND	ND
15	ND	ND	ND	ND	ND	ND	wt
19	ND	ND	ND	ND	ND	ND	wt

[a]ND, not determined

Table 2

Chromosomal aberrations from SKY analysis

Tumor sample	# Cells	Average # aberrations per cell (± CI 95%)		
		Chromosomes	Translocations	Deletions/Duplications
***Msh3*$^{-/-}$ *p53*$^{-/-}$**	23	55[a] (51–83)	1.2 (0.4–1.9)	1.0 (0.4–1.5)
***Msh2*$^{-/-}$ *p53*$^{-/\−}$**	26	40 (39–41)	0.9 (0.5–1.3)	0.7 (0.2–1.2)
***p53*$^{-/-}$**	17	51 (51–54)	0.5 (0.1–0.8)	1.2 (0.4–1.9)

[a] both *Msh3*$^{-/-}$*p53*$^{-/-}$ ($p < .001$) and *p53*$^{-/-}$ ($p = .001$) tumors have significantly more chromosomes per cell compared with *Msh2*$^{-/-}$*p53*$^{-/-}$ tumor cells